annalen der physik

www.ann-phys.org

$L1_0$ Stacked Binaries as Candidates for Hard-Magnets: FePt, MnAl and MnGa

Yu-ichiro Matsushita, Galia Madjarova, José A. Flores-Livas, J. K. Dewhurst, C. Felser, S. Sharma, and E. K. U. Gross*

We present a novel approach for designing new hard magnets by forming stacks of existing binary magnets to enhance the magneto crystalline anisotropy. This is followed by an attempt at reducing the amount of expensive metal in these stacks by replacing it with cheaper metal with similar ionic radius. This strategy is explored using examples of FePt, MnAl and MnGa. In this study a few promising materials are suggested as good candidates for hard magnets: stacked binary $FePt_2MnGa_2$ in structure where each magnetic layer is separated by two non-magnetic layers, FePtMnGa and FePtMnAl in hexagonally distorted Heusler structures and $FePt_{0.5}Ti_{0.5}MnAl$.

1. Introduction

The importance of magnets for modern society can hardly be overstated; they enter into every walk of life from medical equipment to transport (trains, planes, cars) to electronic appliances (from household equipment to computers). All these devices use what is known as hard magnets. The most prominent examples of hard magnets are $Nd_2Fe_{14}B$, $SmCo_5$ and Sm_2Co_{17}. These materials are the strongest permanent magnets known to date.[1–5] Rare-earth metals (REM) are, however, expensive and extracting them from mined ore is a highly polluting process.[6] It is therefore highly desirable to find a new generation of hard magnets that contain less or no rare-earth atoms.[5,7–9]

The first natural question to ask for designing new hard magnets is "what makes the existing permanent magnets hard from a microscopic point of view?" For a magnet to be useful it needs to have two qualities (a) large saturation magnetization density (M_s) and (b) a large magneto-crystalline anisotropy (MCA). A large MCA is needed to make a magnet stable with respect to external influences such as magnetic fields.[10] The large magnetization density in these rare-earth magnets is provided by the ferromagnetic coupling between the magnetic atom (Fe, Co or Sm), while the large MCA is due to both to the low symmetry of the crystal structure and the large spin-orbit coupling provided by the localized f-electrons. Thus, in order to design rare-earth free hard magnets one needs primarily to rely on low symmetry of the crystal structure to achieve large MCA since the spin-orbit coupling is considerably smaller in d-electron materials.[11]

There exist several strategies to design new hard magnets; in the present work we explore a novel idea: step 1. identify two existing binary compounds with desirable magnetic properties (with large M_s and crystallizing in structures with high MCA); step 2. stack these compounds together to form super-structures leading to further enhancement in the MCA; and finally step 3. identifying the expensive component of this stack and attempt to reduce it. This combination of the two binaries reminds one of the quaternary Heuslers of the type XX'YZ where atoms X, X' and Y are d-elements, the atom Z is a p-element with metallic character.[12–16] Quaternary Heusler structures are mainly investigated as half-metallic ferro-magnets[17–22] and are yet to be investigated from the viewpoint of hard magnetic materials.

In the present work we explore the above mentioned strategy by identifying FePt and MnAl (or MnGa) as the binary compounds. These materials have $L1_0$ structure with large MCA.[23,24] The minimum energy and structures close-by for the stacks of these $L1_0$ magnets are then explored for ferromagnetically coupled materials with large M_s. We have also explored quaternary (un)distorted Heusler structures for these materials. The most expensive component of these compounds is Pt. We then look for possible ways to reduce the amount of Pt. In doing so we identify a few candidates for hard magnets; stacked structure of $FePt_2MnGa_2$, FePtMnAl and FePtMnGa in hexagonally distorted Heusler structure and $FePt_{0.5}Ti_{0.5}MnAl$.

Y. Matsushita, G. Madjarova, J. K. Dewhurst, S. Sharma, E. K. U. Gross
Max-Planck Institut für Microstrukture Physics
Weinberg 2, 06120 Halle, Germany
E-mail: matsushita@ap.t.u-tokyo.ac.jp

Y. Matsushita
Department of Applied Physics
The University of Tokyo
Tokyo 113-8656, Japan

G. Madjarova
Department of Physical Chemistry, Faculty of Chemistry and Pharmacy
Sofia University
1126 Sofia, Bulgaria

J. A. Flores-Livas
Department of Physics
Universität Basel
Klingelbergstr. 82, 4056 Basel, Switzerland

C. Felser
Max Planck Institute for Chemical Physics of Solids
Nöthnitzer Strasse 40, 01187 Dresden, Germany

S. Sharma
Department of Physics
Indian Institute of Technology
Roorkee, 247667 Uttarkhand, India

DOI: 10.1002/andp.201600412

© 2017 by WILEY-VCH Verlag GmbH & Co. KGaA, Weinheim

TH-2017-36

2. Computational Details

Full geometry optimization for all materials was performed using the Vienna ab-initio Simulation Package (VASP) with PAW pseudo potential method[25] using PBE exchange-correlation potential.[26] The energy cutoff of 400 eV and a Γ-centered Monkhorst-Pack 10 × 10 × 10 (8 × 8 × 8) *k*-point grid was used for cubic and tetragonal (hexagonal) structures. Spin-orbit coupling (SOC) and fully non-collinear magnetic structure calculations was employed in all our studies in order to explore all possible spin configurations. Accuracy of the electronic ground state and the magneto-crystalline anisotropy calculations was set to be 10^{-7} eV. Such fully non-collinear calculations require highly accurate all electron method; full potential linearized augmented-plane wave (FP-LAPW) method as implemented within the Elk code[27] was used. The definition of the calculated MCA is

$$\mathrm{MCA} = E^{\mathrm{tot}}_{[100]} - E^{\mathrm{tot}}_{[001]},$$

where $E^{\mathrm{tot}}_{[100]}$ ($E^{\mathrm{tot}}_{[001]}$) is the total energy with the spin orientation along the [100] ([001]) direction. Negative values of MCA indicate in-plane spin direction and positive values - out-of-plane. For MCA calculations, we used 15×15×15 sampling k-points to assure the accuracy.

3. Results and Discussion

3.1. Stacked $L1_0$ Structures

As a first step we look at various stacked $2\times L1_0$ structures of FePt-MnAl and FePt-MnGa. The development of the layered-crystal-fabrication technique makes it possible to control the stacking of layers on an atomic scale. Using such techniques, several complex layered magnetic materials are already reported in the literature.[28–30] The investigated stacked $L1_0$ structures are shown in **Figure 1**. Structures A1 and A2 compose of two different stacking sequences of atomic planes; Fe or Pt terminated FePt on MnGa. Structures B1, B2, B3 and B4 are built by stacking in [001] direction Fe or Pt rich FePt on Mn or Ga rich MnGa.

The results are shown in **Figure 2** and **Table 1**. Energy gain compared with the each constituent-simple substance, called formation energy E^{form}, is also shown in Table 1; $E^{\mathrm{form}} \equiv E^{\mathrm{compound}} - \sum E^{\mathrm{simple}}$, where E^{compound} (E^{simple}) is the total energy of the compound (simple substance). Negative values of the formation energy mean that compound materials are energetically favorable than simple substances. As clearly shown in Table 1, most materials prefer compound except for Str. B3. Stability of the studied structures against disorder and high temperature phase separation channels is not explored in this article.

We have calculated only one case of phase separation; decomposition to 2 binaries.The phase separation energy difference is defined: $E^{\mathrm{ph.s}} \equiv E^{\mathrm{compound}} - \sum E^{\mathrm{binary}}$, where the E^{binary} represents total energy of binary alloys, i.e., FePt, MnGa, or MnAl. From Table 1, we have found that FePtMnAl in Str.A2 is more stable than 2 binaries.

Structures A1 and A2 show ferri-magnetic coupling between Mn and Fe atoms which results in a very small total moment. Structure B1, B2 and B3 also show ferri-magnetic coupling between the two magnetic species. This renders all these structure types inappropriate for the purpose of hard magnets.

$L1_0$ structured binary compounds that are building blocks of our new proposed structures have high Ms and MCA values: FePt (Ms = 1130 kA/m, MCA = 6.6 MJ/m^3),[31] MnAl (Ms = 600 kA/m, MCA = 1 MJ/m^3),[32] and MnGa (Ms = 650 kA/m, MCA = 1.6 MJ/m^3)[33] in experimental values make them hard magnets. The most interesting stacked structure type turns out to be structure B4 where the magnetic atoms are separated by two layers of non-magnetic atoms. For this structure type ferromagnetic ordering with a large magnetic moment is obtained (magnetic moments at Fe and Mn sites are 3.07 and 2.28 μ_B respectively). Before the calculations of MCA, we performed detailed convergence test with respect to the number of k-points presented in **Figure 3**. As one can see, the chosen grid, i.e., 15×15×15, is reliable for calculating MCA values. The calculated MCA, in B4 structure, is −5.06 [MJ/m^3] for $FePt_2MnGa_2$ and −0.84 [MJ/m^3] for $FePt_2MnAl_2$ making the former comparable to the binaries and identifying it as a good candidate for hard magnet (See **Table 2**). To assure the stability of these materials in B4 structure, we have calculated the total energy differences between the B4 structure and the constituent $L1_0$ binaries+pure-Pt+pure-Ga(Al). The calculated values are as follows: −1.233 (eV) for $FePt_2MnGa_2$, and −2.037 (eV) for $FePt_2MnAl_2$, where negative values indicate that the stacked binaries are stabler than the decomposed $L1_0$ binaries.

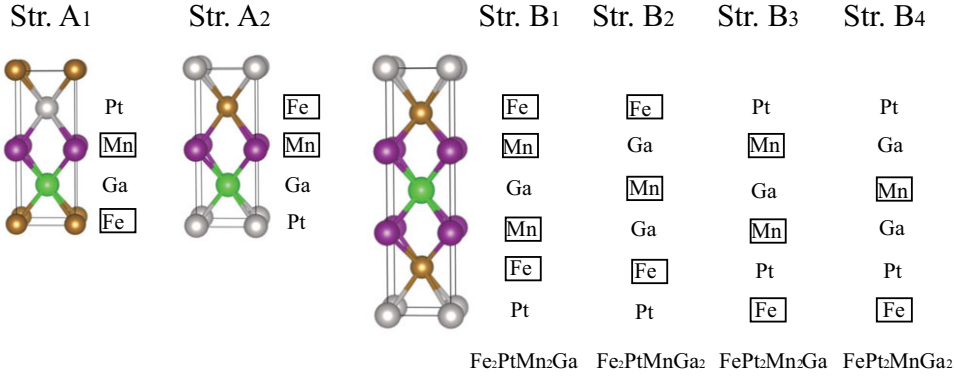

Figure 1. Stacked $L1_0$ structures of FePtMnGa. Various stacking sequences leading to different poly-types. Magnetic layers are marked by squares.

© 2017 by WILEY-VCH Verlag GmbH & Co. KGaA, Weinheim

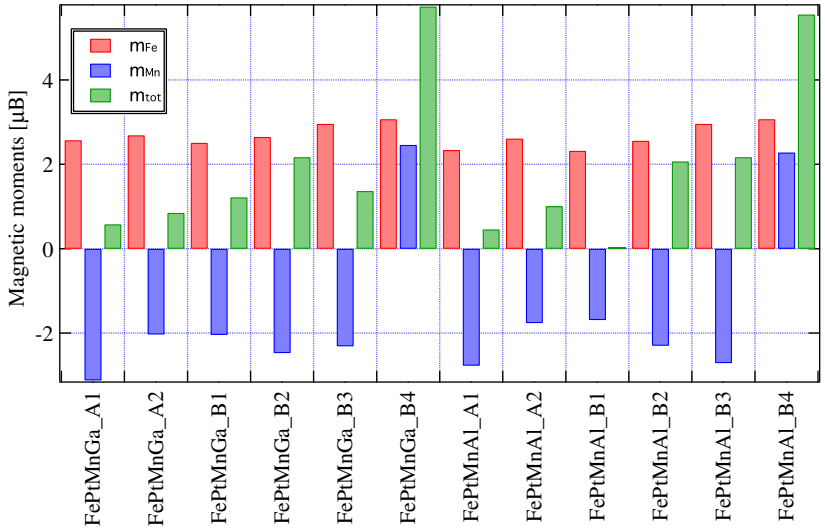

Figure 2. Calculated magnetic moments in μ_B for different layered structures of FePtMnGa and FePtMnAl. The magnetic moments at Fe and Mn sites are shown in red and blue bars, respectively. Green bars represent total magnetic moments per formula unit.

Table 1. Calculated magnetic moments in μ_B for different layered structures of FePtMnGa and FePtMnAl. m_{Fe} and m_{Mn} show the magnetic moments at Fe, and Mn sites, respectively. m_t is the total magnetic moment. Formation energy per formula unit, E^{form}[eV], phase separation energy to 2 binary compounds, $E^{ph.s}$[eV], are also shown.

FePtMnGa	m_{Fe}	m_{Mn}	m_{Mn}	m_{Fe}	m_t [μ_B]	E^{form}[eV]	$E^{ph.s}$
Str. A1	2.57	−3.12	–	–	0.58	−1.012	0.07
Str. A2	2.69	−2.03	–	–	0.85	−0.971	0.12
Str. B1	2.51	−2.04	−2.04	2.51	1.22	−0.934	–
Str. B2	2.65	−2.47	–	2.47	2.17	−5.013	–
Str. B3	−2.96	2.31	2.31	–	1.37	2.782	–
Str. B4	3.07	2.46	–	–	5.74	−2.326	–
FePtMnAl	m_{Fe}	m_{Mn}	m_{Mn}	m_{Fe}	m_t [μ_B]	E^{form}[eV]	$E^{ph.s}$
Str. A1	2.34	−2.77	–	–	0.46	−1.134	0.02
Str. A2	2.61	−1.76	–	–	1.01	−1.430	−0.27
Str. B1	−2.32	1.69	−1.69	2.32	0	−1.043	–
Str. B2	2.41	2.30	–	−2.56	2.07	−5.055	–
Str. B3	−2.96	2.71	2.71	–	2.17	1.608	–
Str. B4	3.07	2.28	–	–	5.55	−3.215	–

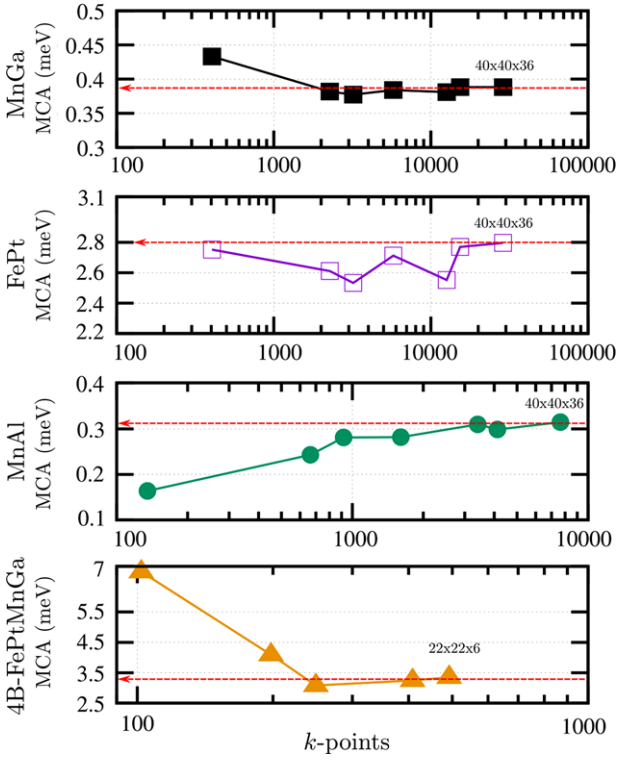

Figure 3. Calculated MCA for $L1_0$-MnGa, FePt, MnAl, and B4-FePtMnGa as a function of the number of k-points in the irreducible Brillouin zone. Indicated in with red-dashed line the converged value and the largest $k-$mesh calculated is indicated.

3.2. Distorted and Undistorted Quaternary Heusler Structures

Since structures A1 and A2 are stoichiometrically identical to the quaternary Heusler structures, we also study these structures. There are three quaternary Heusler structures[34,35] based on the different positions of the atoms (see **Table 3** and **Figure 4** for details).

We find that as compared to the structures A1 and A2, the cubic quaternary Heusler structures are ∼400 meV/f.u. lower in energy. The calculated optimized lattice constant ration, relative total energies and the magnetic moment on each site are presented in **Table 4**. It is clear from these results that for both materials the most stable structure is type I (cubic structure) with ferromagnetic coupling between the magnetic atoms. These results are in a good agreement with previously investigated quaternary Heusler compounds.[12,22] The calculated magnetic moment is around $4\mu_B$ per formula unit which is in good agreement with the Slater-Pauling rule[36,37]: $M_t = Z_t - 24$ where M_t is total spin

© 2017 by WILEY-VCH Verlag GmbH & Co. KGaA, Weinheim

Table 2. Comparison of $FePt_2MnAl_2$ and $FeTi_2MnAl_2$.

	m_{Fe}	m_{Mn}	m_t [μ_B]	MCA [MJ/m^3]	M_s [kA/m]
$FePt_2MnAl_2$	3.07	2.28	5.55	−0.84	615
$FeTi_2MnAl_2$	0.04	2.00	2.23	0.32	300
$FePt_2MnGa_2$	3.07	2.46	5.74	−5.06	617
$FeTi_2MnGa_2$	0.09	2.72	2.77	0.59	307

Table 3. Three different types of atomic arrangement in the quaternary Heusler compound XX'YZ with the space group F-43m.

$F-43m$	4a	4c	4b	4d
	(0,0,0)	(1/4,1/4,1/4)	(1/2,1/2,1/2)	(3/4,3/4,3/4)
type I	Z	X'	Y	X
type II	Z	Y	X'	X
type III	Z	Y	X	X'

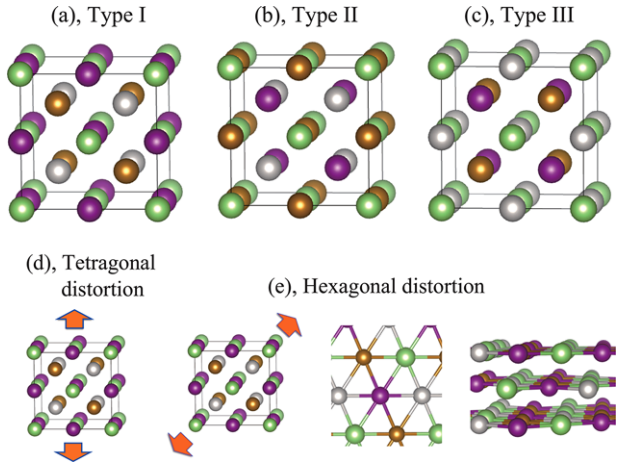

Figure 4. Three possible quaternary Heusler structures (a)-(c), denoted TypeI-III (See Text and Table 4 for details). (d) and (e) represent two possible distortions of the cubic structure namely tetragonal (d) and hexagonal (e). In these figures, different colours of balls depict X, X', Y, and Z element.

moment and Z_t is total number of valence electrons which is 28 for these materials. Despite large magnetic moment, cubic symmetry in these materials leads to very small MCA rendering them bad candidates for hard magnets.

Structural optimization of Heusler structures of type II and III show that tetragonal distortion is favorable (these structures are what is known as $D0_{22}$). Here we can see big differences in the properties of the two investigated materials: for FePtMnGa structures II and III are ∼94 meV/f.u higher in energy than the cubic structure type I and have ferromagnetic ordering. While for FePtMnAl this energy difference is ∼300 meV/f.u. From the viewpoint of formation and phase separation energy, all of them take negative values, which means these compounds are stable than simple substances and binaries. These results are particularly interesting because such tetragonal distortion is highly desirable as it leads to an increase in the MCA. We can see clear relation between MCA and tetragonal distortion (i.e. $c/a > 1$) in the Table 4. The calculated MCA values in cubic structure type I are zero while high MCA values are obtained for structure type II and III. However, the easy axis in most of these materials is in-plane making them bad candidates for hard magnets.

Although cubic structure is global minimum for all the quaternary Heusler structures studied in the present work, we find hexagonal distortion to be very close in energy to the cubic ground-state for both FePtMnGa and FePtMnAl (see Figure 4, and **Table 5**). Such hexagonal phase has been experimentally observed in a similar material,[38] Mn_2TiSn, and in a few materials of the special family X_3Z. Most importantly, we find high MCA values of 3.72 [MJ/m^3] for FePtMnGa and 3.24 [MJ/m^3] for FePtMnAl (see Table 4) with the easy axis in z-direction making these materials very good candidates for hard magnets.

The calculated values for hexagonal FePtMnGa(Al) for M_s and MCA are comparable to the values observed for the current state-of-the-art hard-magnets. For instance, important materials such as YCo_5 have values $M_s = 850$ kA/m and $K_1 \sim 6.5$ MJ/m^3 and $SmCo_{17}$ have $M_s = 970$ kA/m and $K_1 \sim 4.2$ MJ/m^3. Even XXX has substantially improved values specially when compared to widely use oxide-ferrite-based magnets, $BaFe_{12}O_{19}$ for instance with $M_s = 380$ kA/m and $K_1 \sim 0.33$ MJ/m^3.

Table 4. Calculated optimized lattice constant ratio c/a, relative energies per formula unit ΔE given in meV, magnetic moments in μ_B, magneto-crystalline anisotropy (MCA) and saturation magnetization density M_s for quaternary FePtMnGa and FePtMnAl structures. Formation energy per formula unit, E^{form}[eV], phase separation energy to 2 binary compounds, $E^{ph.s}$[eV], are also shown.

FePtMnGa	c/a	ΔE [meV]	m_{Fe}	m_{Mn}	m_t [μ_B]	MCA [MJ/m^3]	M_s [kA/m]	E^{form}[eV]	$E^{ph.s}$[eV]
I type	1.0	0	1.10	3.02	4.20	0	730	−1.377	−0.288
II type	1.34	93.27	2.54	3.01	5.67	0.21	973	−1.284	−0.195
III type	1.23	99.77	2.54	3.22	5.83	-4.5	991	−1.278	−0.187
hex	0.77	3.43	2.01	3.03	5.09	3.72	889	−1.374	−0.283
FePtMnAl	c/a	ΔE [meV]	m_{Fe}	m_{Mn}	m_t [μ_B]	MCA [MJ/m^3]	M_s [kA/m]	E^{form}[eV]	$E^{ph.s}$[eV]
type I	1.0	0	0.94	3.00	4.07	0	729	−1.890	−0.714
type II	1.14	294	2.61	2.73	5.52	−2.03	956	−1.596	−0.420
type III	1.43	307	2.43	3.09	5.62	−1.43	974	−1.583	−0.407
hex	0.73	44	1.39	2.91	4.39	3.24	893	−1.846	−0.669

© 2017 by WILEY-VCH Verlag GmbH & Co. KGaA, Weinheim

Table 5. Optimized lattice constant and atomic positions for FePtMnAl and FePtMnGa in hexagonal structure.

hex_FePtMnAl	hex_FePtMnGa
Lattice constant (Å)	
$a = 5.779$, $b = 5.107$, $c = 4.216$	$a = 5.589$, $b = 5.225$, $c = 4.307$
$\alpha = \beta = 90^\circ$, $\gamma = 56.58^\circ$	$\alpha = \beta = 90^\circ$, $\gamma = 57.04^\circ$
Atom positions	
Fe (0.000, 0.559, 0.000)	Fe (−0.023, 0.544, 0.000)
Fe (0.691, 0.108, 0.500)	Fe (0.690, 0.122, 0.500)
Pt (0.472, 0.569, 0.000)	Pt (0.495, 0.525, 0.000)
Pt (0.195, 0.097, 0.500)	Pt (0.172, 0.142, 0.500)
Mn (0.486, 0.067, 0.000)	Mn (0.482, 0.044, 0.000)
Mn (0.181, 0.600, 0.500)	Mn (0.185, 0.622, 0.500)
Al (−0.040, 0.053, 0.000)	Ga (−0.015, 0.018, 0.000)
Al (0.706, 0.613, 0.500)	Ga (0.682, 0.649, 0.500)

3.3. Reducing the Amount of Pt

We now focus upon the issue of reducing the amount of Pt by replacing it with less expensive metals. We have tried 50-100 % substitution of Pt by an element of similar radius (i.e. Ti) in both of the candidates for hard magnets; FePtMnAl and FePtMnGa in structures B4 and (un)distorted quaternary Heusler.

In case of FePtMnAl (in B4 structure), on 100% substitution of Pt by Ti, the magnetic moment on the Mn atom is almost the same because the Mn atom is surrounded by 8 Al atoms and its environment stays unchanged on such a substitution. Unfortunately, the calculated magnetic moment at Fe sites in $FeTi_2MnAl_2$ is almost 0 (see Table 2). Same behaviour is also seen in $FeTi_2MnGa_2$.

In order to understand the reason for this loss in moment on Fe site we compare the density of states (DOS) for $FePt_2MnAl_2$ and $FeTi_2MnAl_2$ (see **Figure 5**). A dramatic change is seen in the partial DOS at the Fe site on replacing Pt by Ti; in the $FePt_2MnAl_2$ a big exchange splitting leads to large moment while in the $FeTi_2MnAl_2$ this exchange splitting almost vanishes making Fe non magnetic. This is mainly due to the fact that electronic states

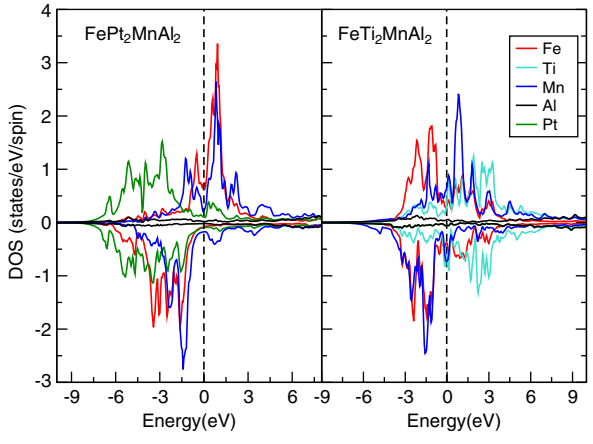

Figure 5. Partial density of states (in states/eV/spin) for $FePt_2MnAl_2$ and $FeTi_2MnAl_2$.

Table 6. Calculated magnetic moments in μ_B, magneto-crystalline anisotropy (MCA), saturation magnetization density M_s, and formation energy E^{form} for structures with 50 % substitution of Pt.

Structure	m_{Fe}	m_{Mn}	m_t [μ_B]	MCA [MJ/m^3]	M_s [kA/m]	E^{form}[eV]
$FePt_{0.5}Ti_{0.5}$MnAl type I	1.67	2.48	4.13	1.27	754	−1.526
$FePt_{0.5}Ti_{0.5}$MnAl hex.	2.08	2.44	4.12	0.79	705	−1.431
$FePt_{0.5}Ti_{0.5}$MnGa type I	AFM	AFM	AFM	–	54	−1.572
$FePt_{0.5}Ti_{0.5}$MnGa hex.	2.16	2.59	4.29	0.11	730	−1.350

at Fe sites (symmetry of D_{4h}) are strongly affected by crystal field from Ti sites. The *d*-electrons are split into 4 irreducible subgroups, i.e., $\{d_{yz}\ d_{zx}\}$, $\{d_{z^2}\}$, $\{d_{xy}\}$, $\{d_{x^2-y^2}\}$. In $FeTi_2MnAl_2$, six *d*-electrons of Fe occupy first three orbitals, showing very little magnetic moment. On the other hand, in the $FePt_2MnAl_2$, the effect of exchange splitting and spin-orbit interaction is much stronger than the crystal field splitting, leading to a large moment on the Fe sites (see Figure 5). This indicates that Fe atoms at D_{4h} sites surrounded by early transition elements are not favorable candidates for hard magnets. To test this hypothesis further we have substituted Pt sites with late transition elements (like Ir and Au) and we find that the moment is recovered (to 2.9 μ_B for Ir, and 2.5 μ_B for Au) and a large MCA is obtained. Hence these materials would make excellent hard magnets. However, Ir and Au are almost as expensive as Pt and such a replacement is not useful from economical point of view.

For the case of quaternary Heusler structure we have explored the possibility of 50% substitution of Pt sites with Ti. This is achieved by making a 2x2x2 super-cell in which the Ti atoms are located such that two neighboring Ti atoms are maximally separated. The results are shown in **Table 6**. A full structural optimization shows that type I structure is the most stable. Owing to the 50 % substitution, the cubic symmetry around the magnetic atoms is broken and high MCA value is obtained. Another good point is its negative formation energy, which means the compound is stabilized by −1.377 (eV) for FePtMnGa, and −1.890 (eV) for FePtMnAl. Unfortunately, $FePt_{0.5}Ti_{0.5}$MnGa shows AFM ordering and hence is not a useful candidate, but $FePt_{0.5}Ti_{0.5}$MnAl is FM with large MCA of 1.27 [MJ/m^3] making it a strong candidate for hard magnet.

Possibility for 50 % substitution of Pt was also checked in the hexagonal structure (see Table 6). Magnetization remains the same but MCA value reduces compered to the other structures. All promising candidates are presented **Figure 6**.

4. Summary

To summarize, we presented a novel approach towards designing new hard magnets; making stacks of already existing binary magnets to enhance the MCA. This is followed by an attempt at reducing the amount of expensive metal in these stacks by replacing it with cheaper metal with the same ionic radius. This strategy was explored using existing $L1_0$ binaries MnPt, MnGa and MnAl and in doing so we have identified few possible candidates for hard magnets: FePtMnGa and FePtMnAl in hexagonally distorted Heusler structure, FePtMnGa in B4 structure and $FePt_{0.5}Ti_{0.5}$MnAl. We also note that replacing Pt by Ir or Au leads

© 2017 by WILEY-VCH Verlag GmbH & Co. KGaA, Weinheim

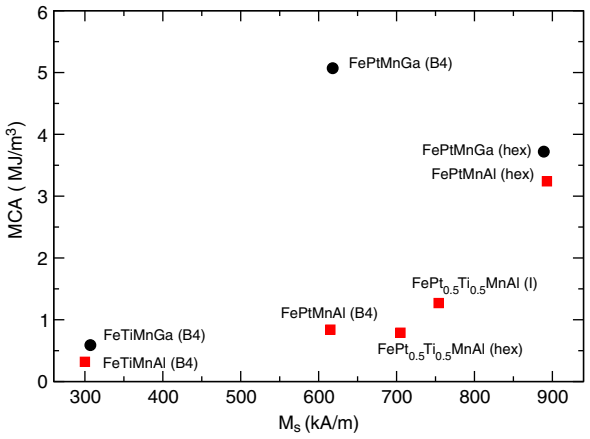

Figure 6. Plotted M_s and absolute MCA values for some candidates as hard magnets proposed in this work.

to excellent candidates for hard magnets in these materials, but since both these metals are as expensive as Pt such a substitution is not useful from economical point of view.

Acknowledgments

J.A.F.-L. acknowledges the financial support from EU's 7th Framework Marie-Curie Program within the "ExMaMa" Project (329386) and computational resources under the project s752 from the Swiss National Supercomputing Center (CSCS) in Lugano. This work has been funded by the Joint Initiative for Research and Innovation within the Fraunhofer and Max Planck cooperation program.

Conflict of Interest

The authors declare no conflict of interest.

Keywords

hard magnets, DFT calculations, L10 binary, Heusler compounds

Received: December 23, 2016
Revised: March 9, 2017
Published online: July 5, 2017

[1] M. Sagawa, S. Fujimura, H. Yamamoto, Y. Matsuura, and K. Hiraga, Magnetics, *IEEE Transactions on* **20**(1584) (1984).
[2] J. F. Herbst, *Rev. Mod. Phys.* **63**(819) (1991).
[3] G. Hoffer and K. Strnat, Magnetics, *IEEE Transactions on* **2**(487) (1966).
[4] H. Senno and Y. Tawara, Magnetics, *IEEE Transactions on* **10**(313) (1974).
[5] J. Coey, *IEEE Transactions on Magnetics* **47**(4671) (2011).
[6] N. available, *EPA* **572**(600) (2012).
[7] R. McCallum, L. Lewis, R. Skomski, M. J. Kramer, and I. Anderson, *Annu. Rev. Mater. Res.* **44**(451) (2014).
[8] J. Coey, *Scripta Materialia* **67**(524) (2012).
[9] M. Kramer, M. R.W., A. I.A., and S. Constantinides, *JOM* **64**(752) (2012).
[10] J. M. Coey, *Magnetism and magnetic materials* (Cambridge University Press, 2010).
[11] R. Skomski and J. Coey, *Permanent magnetism* (Institute of Physics Pub., 1999).
[12] C. S. Lue and Y.-K. Kuo, *Phys. Rev. B* **66**(085121) (2002).
[13] V. Alijani, S. Ouardi, G. H. Fecher, J. Winterlik, S. S. Naghavi, X. Kozina, G. Stryganyuk, C. Felser, E. Ikenaga, Y. Yamashita, S. Ueda, and K. Kobayashi, *Phys. Rev. B* **84**(224416) (2011).
[14] T. Graf, C. Felser, and S. Parkin, *Progress in Solid State Chemistry* **39**(1) (2011).
[15] T. Graf, L. Winterlik, L. Muchler, G. Fecher, C. Felser, and P. S.P., *Handbook of Magnetic Materials* **21**(1) (2013).
[16] G. Kreiner, A. Kalache, S. Hausdorf, V. Alijanin, J.-F. Qian, U. Burkhardt, S. Ouardi, and C. Felser, *Z. Anorg. Allg. Chem* **640**(738) (2014).
[17] G. Gokoglu, *Solid State science* **17**(1273) (2012).
[18] J. Nehra, V. D. Sudheesh, N. Lakshmi, and K. Venugopalan, *Phys. Status Solidi RRL* **7**(289) (2013).
[19] V. Alijani, J. Winterlik, G. H. Fecher, S. S. Naghavi, and C. Felser, *Phys. Rev. B* **83**(184428) (2011).
[20] M. Singh, H. S. Saini, J. Thakur, A. H. Reshak, and M. K. Kashyap, *Journal of Alloys and Compounds* **580**(201) (2013).
[21] J. Zhang, Z. Liu, G. Li, X. Ma, and L. G.D., *Journal of Alloys and Compounds* **616**(449) (2013).
[22] G. Gao, L. Hu, Y. Yao, B. Luo, and N. Liu, *Journal of Alloys and Compounds* **580**(539) (2013).
[23] A. Edström, J. Chico, A. Jakobsson, A. Bergman, and J. Rusz, *Phys. Rev. B* **90**(014402) (2014).
[24] S. Okamoto, N. Kikuchi, O. Kitakami, T. Miyazaki, Y. Shimada, and K. Fukamichi, *Phys. Rev. B* **66**(024413) (2002).
[25] G. Kresse and J. Furthmüller, *Comput. Mat. Sci.* **6**(15) (1996).
[26] J. P. Perdew, K. Burke, and M. Ernzerhof, *Phys. Rev. Lett.* **77**(3865) (1996).
[27] K. Dewhurst, S. Sharma, L. Nordstroem, F. Cricchio, F. Bultmark, O. Granas, E. K. U. Gross, C. Ambrosch-Draxl, C. Persson, Brouder, R. Armiento, P. Chizmeshya, A. Anderson, I. Nekrasov, F. Wagner, J. Kalarasse, Spitaler, S. Pittalis, N. Lathiotakis, T. Burnus, S. Sagmeister, C. Meisenbichler, S. Lebegue, Y. Zhang, Y. Kormann, A. Baranov, A. Kozhevnikov, S. Suehara, F. Essenberger, A. Sanna, T. McQueen, T. Baldsiefen, M. Blaber, T. Filanovich, A. Bjorkman, M. Stankovski, J. Goraus, M. Meinert, D. Rohr, V. Nazarov, K. Krieger, P. Floyd, A. Davydov, F. Eich, K. Romero, A. Kitahara, J. Glasbrenner, K. Bussmann, I. Mazin, M. Verstraete, D. Ernsting, S. Dugdale, P. Elliott, M. Dulak, J. A. Flores-Livas, S. Cottenier, and Y. Shinohara, *The Elk FP-LAPW Code* (2015).
[28] K. Takanashi, S. Mitani, M. Sano, H. Fujimori, H. Nakajima, and A. Osawa, *Appl. Phys. Lett.* **67**(1016) (1995).
[29] S. Gautam, K. Asokan, J. P. Singh, F.-H. Chang, H.-J. Lin, and K. H. Chae, *J. Appl. Phys.* **115**(17C109) (2014).
[30] D. Li, Y. Wang, and Y. Xia, *Advanced Materials* **16**(361) (2004).
[31] D. Weller, A. Moser, L. Folks, M. E. Best, W. Lee, M. F. Toney, M. Schwickert, J. U. Thiele, and M. F. Doerner, *IEEE Transactions on Magnetics* **36**(10) (2000).
[32] M. Hosoda, M. Oogane, M. Kubota, T. Kubota, H. Saruyama, S. Iihama, H. Naganuma, and Y. Ando, *J. Appl. Phys.* **111**(07A324) (2012).
[33] F. W. X. Z. S. Mizukami, T. Kubota and T. Miyazaki, *Physical Review B* **85**(014416) (2012).
[34] U. Eberz, W. Seelentag, and H.-U. Schuster, *Naturforsch.* **35**(1341) (1980).
[35] J. Drews, U. Eberz, and H.-U. Schuster, *J. Less Common Met.* **116**(271) (1986).
[36] J. C. Slater, *Phys. Rev.* **49**(931) (1936).
[37] L. Pauling, *Phys. Rev.* **54**(899) (1938).
[38] P. Kharel, Y. Huh, V. Shah, X. Li, N. Al-Aqtash, K. Tarawneh, E. Krage, R. Sabirianov, R. Skomski, and D. Sellmyer, *J. Appl. Phys.* **111**(07B101) (2012).

© 2017 by WILEY-VCH Verlag GmbH & Co. KGaA, Weinheim